Cardiovascular Revascularization Medicine xxx (xxxx) xxx

Contents lists available at ScienceDirect

Cardiovascular Revascularization Medicine

journal homepage: www.sciencedirect.com/journal/cardiovascular-revascularization-medicine

Reproducibility of an artificial intelligence optical coherence tomography software for tissue characterization: Implications for the design of longitudinal studies

Mohil Garg [a], Hector M. Garcia-Garcia [b,*], Andrea Teira Calderón [c], Jaytin Gupta [d], Shrayus Sortur [d], Molly B. Levine [a], Puneet Singla [a], Andrea Picchi [e], Gennaro Sardella [f], Marianna Adamo [g], Enrico Frigoli [h], Ugo Limbruno [e], Stefano Rigattieri [i], Roberto Diletti [j], Giacomo Boccuzzi [k], Marco Zimarino [l], Marco Contarini [m], Filippo Russo [n], Paolo Calabro [o], Giuseppe Andò [p], Ferdinando Varbella [q], Stefano Garducci [r], Cataldo Palmieri [s], Carlo Briguori [t], Jorge Sanz Sánchez [u,v], Marco Valgimigli [w]

[a] *Department of Internal Medicine, MedStar Washington Hospital Center, Washington, DC, USA*
[b] *Department of Interventional Cardiology, MedStar Washington Hospital Center, Washington, DC, USA*
[c] *Department of Cardiology, Hospital Universitario Marqués de Valdecilla, Santander, Spain*
[d] *Department of Internal Medicine, MedStar Georgetown University Hospital, Washington, DC, USA*
[e] *Misericordia Hospital, Grosseto, Italy*
[f] *Policlinico Umberto I, Sapienza University of Rome, Rome, Italy*
[g] *Azienda Ospedaliera Spedali Civili, Brescia, Italy*
[h] *Clinical Trials Unit, University of Bern, Bern, Switzerland*
[i] *Sandro Pertini Hospital, Rome, Italy*
[j] *Thoraxcenter, Erasmus Medical Center, Rotterdam, the Netherlands*
[k] *San Giovanni Bosco Hospital, Turin, Italy*
[l] *Università degli Studi "G. d'Annunzio" Chieti e Pescara, Chieti, Italy*
[m] *Ospedale Umberto I, Siracusa, Italy*
[n] *Azienda Ospedaliera Sant'Anna, Como, Italy*
[o] *Division of Cardiology, Department of Cardiothoracic and Respiratory Sciences, University of Campania "Luigi Vanvitelli", Naples, Italy*
[p] *Azienda Ospedaliera Universitaria G. Martino, Messina, Italy*
[q] *Cardiology Unit, Ospedali Riuniti di Rivoli, ASL Torino 3, Turin, Italy*
[r] *Unita' Operativa Complessa di Cardiologia ASST di Vimercate (MB), Vimercate, Italy*
[s] *Institute of Clinical Physiology, C.N.R./G. Monasterio Foundation, Massa, Italy*
[t] *Clinica Mediterranea, Napoli, Italy*
[u] *Centro de Investigación Biomedica en Red (CIBERCV), Madrid, Spain*
[v] *Hospital Universitari i Politecnic La Fe, Valencia, Spain*
[w] *Swiss Cardiovascular Center Bern, Bern University Hospital, Freiburgstrasse 8, Bern, Switzerland*

ARTICLE INFO

Keywords:
Optical coherence tomography
OCT
Artificial intelligence

ABSTRACT

Background: To assess the reproducibility of coronary tissue characterization by an Artificial Intelligence Optical Coherence Tomography software (OctPlus, Shanghai Pulse Medical Imaging Technology Inc.).
Methods: 74 patients presenting with multivessel ST-segment elevation myocardial infarction (STEMI) underwent optical coherence tomography (OCT) of the infarct-related artery at the end of primary percutaneous coronary intervention (PPCI) and during staged PCI (SPCI) within 7 days thereafter in the MATRIX (Minimizing Adverse Hemorrhagic Events by Transradial Access Site and angioX) Treatment-Duration study (ClinicalTrials.gov, NCT01433627). OCT films were run through the OctPlus software. The same region of interest between either side of the stent and the first branch was identified on OCT films for each patient at PPCI and SPCI, thus generating 94 pairs of segments. 42 pairs of segments were re-analyzed for intra-software difference. Five plaque

* Corresponding author at: Section of Interventional Cardiology, MedStar Washington Hospital Center, 110 Irving Street, NW, Washington, D.C. 20010, USA.
E-mail address: hector.m.garciagarcia@medstar.net (H.M. Garcia-Garcia).

https://doi.org/10.1016/j.carrev.2023.07.003
Received 18 January 2023; Received in revised form 15 June 2023; Accepted 12 July 2023
Available online 16 July 2023

characteristics including cholesterol crystal, fibrous tissue, calcium, lipid, and macrophage content were analyzed for various parameters (span angle, thickness, and area).

Results: There was no statistically significant inter-catheter (between PPCI and SPCI) or intra-software difference in the mean values of all the parameters. Inter-catheter correlation for area was best seen for calcification [intraclass correlation coefficient (ICC) 0.86], followed by fibrous tissue (ICC 0.87), lipid (ICC 0.62), and macrophage (ICC 0.43). Some of the inter-catheter relative differences for area measurements were large: calcification 9.75 %; cholesterol crystal 74.10 %; fibrous tissue 5.90 %; lipid 4.66 %; and macrophage 1.23 %. By the intra-software measurements, there was an excellent correlation (ICC > 0.9) for all tissue types. The relative differences for area measurements were: calcification 0.64 %; cholesterol crystal 5.34 %; fibrous tissue 0.19 %; lipid 1.07 %; and macrophage 0.60 %. Features of vulnerable plaque, minimum fibrous cap thickness and lipid area showed acceptable reproducibility.

Conclusion: The present study demonstrates an overall good reproducibility of tissue characterization by the Artificial Intelligence Optical Coherence Tomography software. In future longitudinal studies, investigators may use discretion in selecting the imaging endpoints and sample size, accounting for the observed relative differences in this study.

1. Introduction

Optical Coherence Tomography (OCT) provides an unparalleled high-resolution tomographic image of the coronary vessel wall [1]. This helps to delineate the atherosclerotic plaque characteristics such as lipid, calcification, fibrous cap, cholesterol crystals and macrophage infiltration [2–5]. Therefore, this imaging modality has been used in several recent clinical studies assessing the impact of medical therapies on plaque progression [6–10].

One of the major hindrances to the widespread use of OCT is the manual interpretation of OCT images by expert analysts, making it time-consuming and susceptible to intra-observer and inter-observer variability. A potential method to overcome this obstacle is to incorporate automated software to analyze the OCT films. OctPlus (developed by

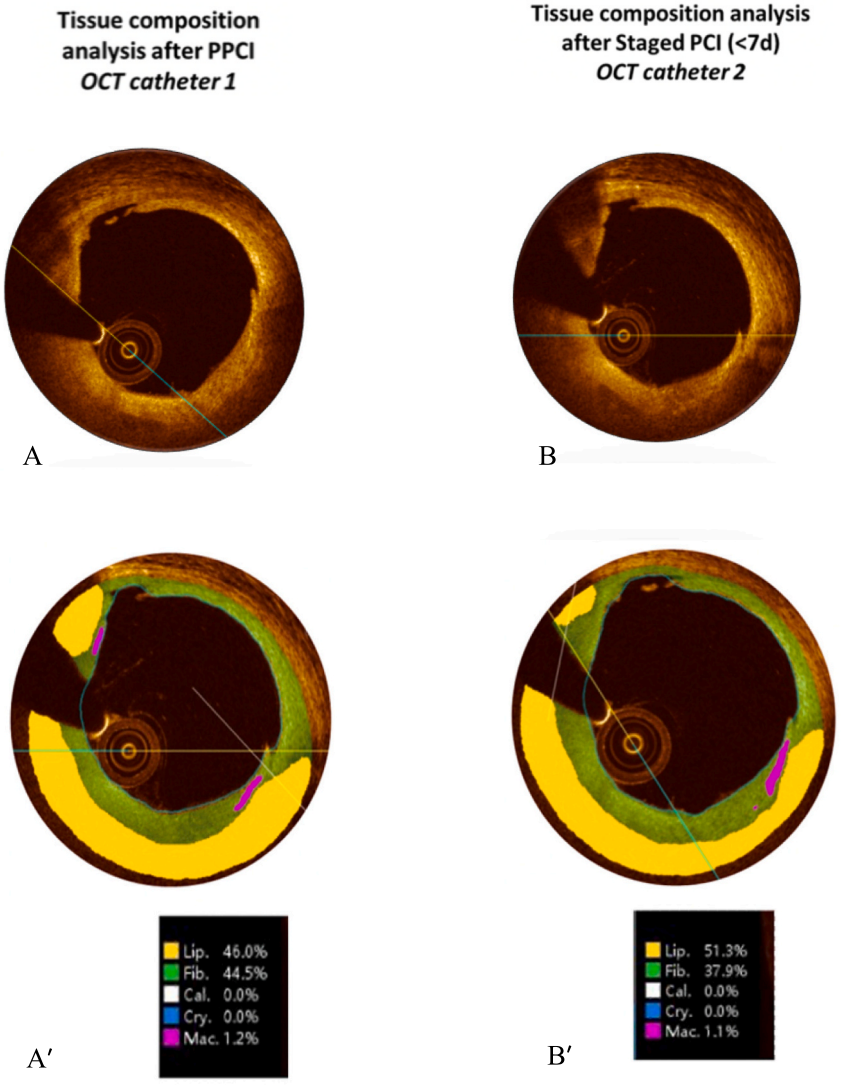

Fig. 1. Example showcasing OCT image interpretation by the OctPlus software.
The OctPlus software color codes plaque characteristics, lipid: yellow, green: fibrous tissue, white: calcium, blue: cholesterol crystal, pink: macrophage. A: OCT image acquired at PPCI; A′: Image A with automatic interpretation by the software; B: OCT image of the same segment as A acquired at Staged PCI which was done within 7 days of PPCI; B′: Image B with automatic interpretation by the software. Plaque erosion can be seen at 11 o' clock position on A and B. Some macrophages seen at 10 o' clock position in A′ are not seen at B′. PPCI: Primary Percutaneous Coronary Intervention. (For interpretation of the references to color in this figure legend, the reader is referred to the web version of this article.)

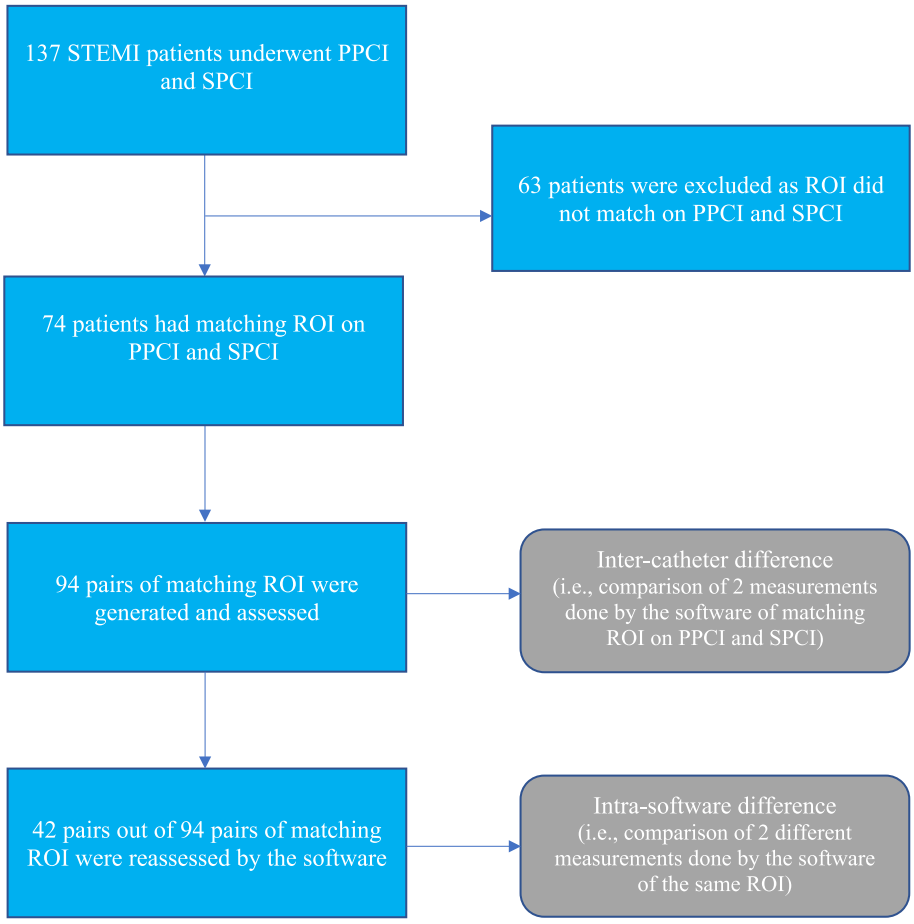

Fig. 2. Flow diagram depicting study design.
STEMI: ST-segment elevation myocardial infarction; ROI: Region of interest; PPCI: Primary Percutaneous Coronary Intervention; SPCI: Staged Percutaneous Coronary Intervention.

Table 1
Characteristics of the patients at baseline.[a]

Characteristic	
Age[b]	61.8 ± 12.9
Male sex	62 (83.7)
Mean weight	77.9 ± 10.8
Body mass index[c]	
Mean	26.5 ± 2.8
≥ 25	48 (64.8)
Diabetes mellitus	11 (14.8)
Smoker	38 (51.3)
Hypercholesterolemia	28 (37.8)
Hypertension	41 (55.4)
Family history of CAD	26 (35.1)
Previous MI	1 (1.3)
Previous CABG	0
Previous TIA or stroke	2 (2.7)
Peripheral vascular disease	3 (4.0)
COPD	1 (1.3)
Renal failure	1 (1.3)

Other characteristics are listed as n (%), Total $N = 74$.
CAD denotes coronary artery disease, MI myocardial infarction, CABG coronary artery bypass grafting, TIA transient ischemic attack, COPD chronic obstructive pulmonary disease.
[a] Plus-minus values are means ± SD.
[b] Age is listed in years.
[c] Body mass index is the weight in kilograms divided by the square of the height in meters.

Shanghai Pulse Medical Imaging Technology Inc.) is one such novel automated software developed for the tissue quantitative and qualitative analysis of the OCT data [11–13]. However, no study has been done to date to assess the validity of tissue characterization measurements by the software. Through this study, the authors intend to analyze the reproducibility of the plaque composition quantification by the OctPlus software in patients studied with 2 different OCT catheters within a week in which it is assumed that no biological variability is present in the coronary vessel wall. This evaluation is essential before it can be used in clinical practice and future studies.

2. Methods

2.1. Study population

Patients presenting with multivessel STEMI who (a) underwent primary percutaneous coronary intervention (PPCI) and a staged percutaneous coronary intervention (SPCI) before discharge and (b) underwent OCT imaging of the infarct related artery at both times. Patients were recruited from the MATRIX (Minimizing Adverse Haemorrhagic Events by TRansradial Access Site and angioX) Treatment-Duration study. MATRIX trial is a multicenter, prospective, open-label, factorial, randomized trial, which compared the effectiveness and safety of unfractionated heparin with glycoprotein IIb/IIIa inhibitors (GPI) versus bivalirudin in patients affected by either non-ST elevation acute coronary syndrome or STEMI (ClinicalTrials.gov, NCT01433627) [14]. SPCI was performed within 7 days of PPCI in all the patients in the MATRIX trial.

Table 2
Mean comparison of different plaque characteristics of matched ROI between PPCI and SPCI i.e., inter-catheter mean difference (n = 94).

	PPCI	SPCI	Absolute difference (PPCI-SPCI)	Relative difference	P value
Calcification					
Span angle (°)	24.86±16.00	25.25±21.28	0.15±12.33	1.57 %	0.92
Thickness (mm)	0.34±0.19	0.34±0.19	0.00±0. 13	1.33 %	0.81
Area (mm^2)	0.26±0.28	0.28±0.34	−0.02±0. 16	9.75 %	0.30
Cholesterol crystal					
Span angle (°)	7.60±3.28	13.10±52.04	−6.67±55.77	72.33 %	0.32
Thickness (mm)	0.09±0.02	0.14±0.50	−0.06±0. 53	60.95 %	0.302
Area (mm^2)	0.01±0.00	0.02±0.09	−0.01±0. 09	74.10 %	0.29
Fibrous tissue					
Span angle (°)	309.9±48.82	312.34±46.38	−2.40±34.39	0.78 %	0.49
Thickness (mm)	0.90±0.17	0.91±0.17	−0.00±0. 13	0.21 %	0.89
Area (mm^2)	3.28±1.26	3.47±1.43	−0.19±0. 68	5.90 %	0.07
Cap thickness (μm)	281.28±10.23	290.42±10.59	−9.14±8.04	3.25 %	0.25
Lipid					
Span angle (°)	66.98±27.48	66.40±28.07	0.28±24.38	0.87 %	0.91
Thickness (mm)	0.55±0.14	0.54±0.15	0.00±0. 11	1.27 %	0.67
Area (mm^2)	0.82±0.44	0.86±0.51	−0.04±0. 41	4.66 %	0.33
Macrophage					
Span angle (°)	16.28±8.07	15.90±6.65	0.36±7.31	2.37 %	0.65
Thickness (mm)	0.11±0.04	0.11±0.03	−0.00±0. 03	0.44 %	0.83
Area (mm^2)	0.03±0.02	0.03±0.01	0.00±0. 02	1.23 %	0.91

Values are mean±SD; ROI: Region of interest; PPCI: Primary Percutaneous Coronary Intervention; SPCI: Staged Percutaneous Coronary Intervention; Absolute difference was calculated as mean difference between PPCI and SPCI; Relative difference was calculated as [1-(SPCI/PPCI)]x100%; P value for comparison between PPCI and SPCI values.

Table 3
Correlation between PPCI and SPCI for different plaque characteristics i.e., inter-catheter correlation (n = 94).

Plaque characteristic	ICC	P value	95 % CI
Calcification			
Span angle	0.78	<0.001	0.70–0.87
Thickness	0.74	<0.001	0.65–0.84
Area	0.86	<0.001	0.81–0.92
Cholesterol crystal			
Span angle	0.00	0.50	0.00–0.21
Thickness	0.00	0.50	0.00–0.21
Area	0.00	0.50	0.00–0.21
Fibrous tissue			
Span angle	0.73	<0.001	0.63–0.81
Thickness	0.70	<0.001	0.58–0.79
Area	0.87	<0.001	0.81–0.91
Minimum FCT	0.70	<0.001	0.59–0.80
Lipid			
Span angle	0.61	<0.001	0.46–0.73
Thickness	0.67	<0.001	0.55–0.77
Area	0.62	<0.001	0.48–0.73
Macrophage			
Span angle	0.51	<0.001	0.35–0.66
Thickness	0.57	<0.001	0.43–0.71
Area	0.43	<0.001	0.27–0.61

ICC: Intraclass correlation coefficient; FCT: Fibrous cap thickness. No correlation was seen for cholesterol crystal. Correlation was best seen for calcification followed by fibrous tissue and lipid.

2.2. Optical coherence tomography acquisition

The OCT catheter was advanced into the vessel so that the proximal marker was at least 10 mm downstream from the distal edge of the stent. The coronary artery was flushed with contrast media at 37C and a flush rate of 3 mL/s for the right coronary artery (RCA) and 4 mL/s for the left coronary artery during the automated OCT pullback. The pullback was carried out at a speed of 20 mm/s and 100 fps. At follow-up during SPCI, the same flush settings were repeated as applied during the baseline PPCI imaging procedure.

2.3. Optical coherence tomography analysis

OCT analysis was performed using Artificial Intelligence Optical Coherence Tomography (OctPlus, Shanghai Pulse Medical Imaging Technology Inc.) [11]. A Region of Interest (ROI) was identified using either side of the stent and the first branch as reference on OCT films for each patient at PPCI. The same ROI was identified in the SPCI OCT film using side-by-side longitudinal and cross-sectional, contour-free views. Some patients had 2 matching ROI since both sides of the stent were analyzed. These matching ROIs on PPCI and SPCI were compared to each other, generating 1 set of inter-catheter differences. Subsequently, some OCT films were re-analyzed using the software. They were compared to the previous measurements done by the software, generating 1 set of intra-software (i.e., intra-observer) differences.

Five plaque characteristics were obtained for each OCT analysis. This included cholesterol crystal, fibrous tissue, calcium, lipid, and macrophage content. The software color-coded these plaque characteristics, as seen in Fig. 1. The five characteristics were further analyzed for various parameters [span angle (°), thickness (mm), and area (mm^2)]. Minimum fibrous cap thickness (FCT) was also analyzed at each frame.

2.4. Statistical analysis

The statistical analysis was performed with Stata Statistical Software: Release 16. College Station, TX: StataCorp LLC). Continuous variables are reported as mean ± SD. Comparisons of means between groups were performed with Student *t*-tests. Correlation coefficient and Bland-Altman plots with limits of agreement are provided. A p value of <0.05 was considered statistically significant.

3. Results

All 137 patients from the MATRIX trial were included in our initial

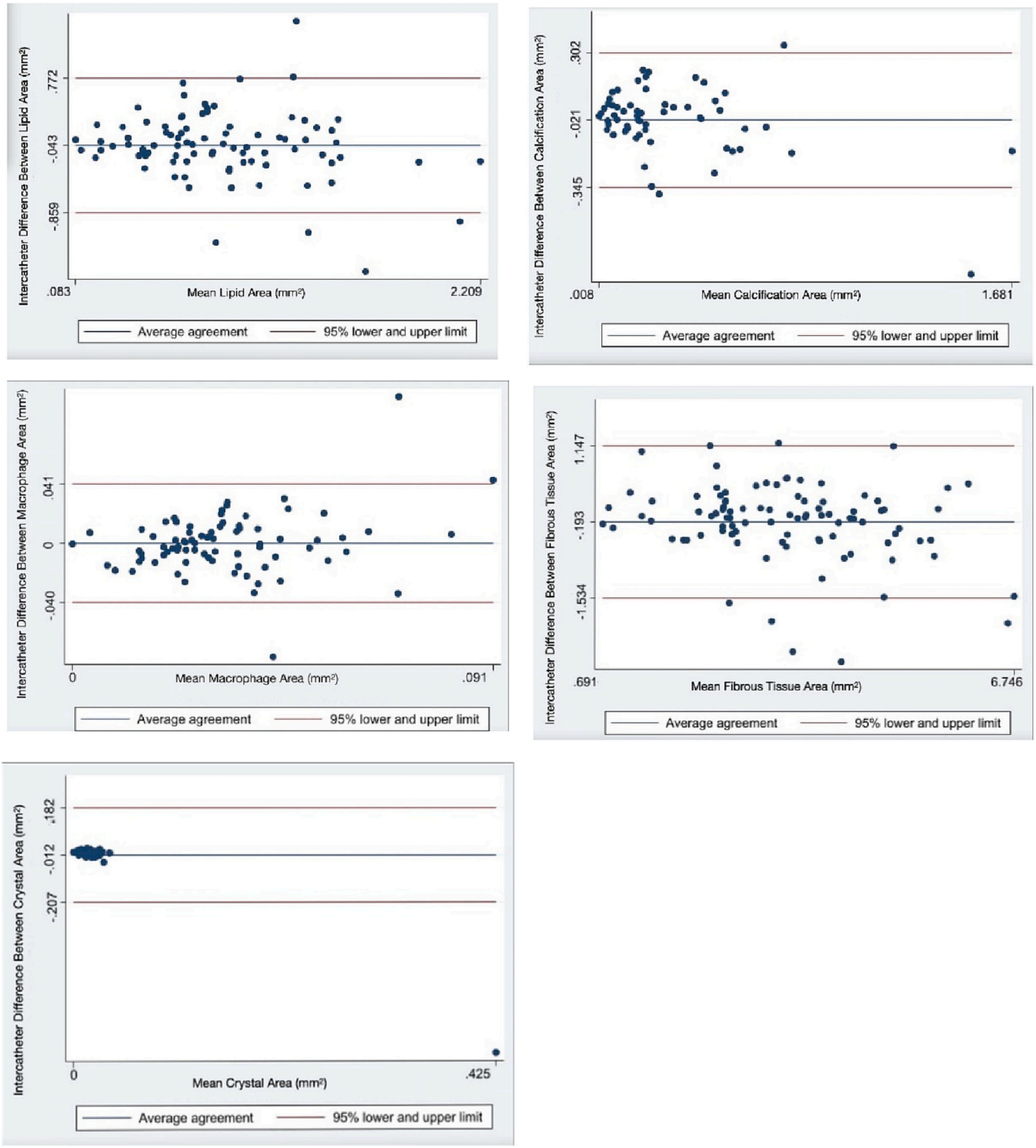

Fig. 3. Bland-Altman plots depicting the agreement between catheters for same region of interest for areas of different plaque characteristics ($n = 94$).

analyses (Fig. 2). 74 patients had 94 pairs of matching ROI on PPCI and SPCI. The remaining 63 patients were excluded due to the lack of pairing data. 21 pairs of segments from both PPCI and SPCI were re-analyzed, generating 42 pairs for intra-software (i.e., intra-observer) difference. The clinical characteristics of 74 patients are summarized in Table 1.

3.1. Inter-catheter agreement

There was no statistically significant inter-catheter difference (between PPCI and SPCI) seen in the mean values of all the parameters (p value >0.05). However, some of the relative differences for area measurements were large between PPCI and SPCI: calcification 9.75 %; cholesterol crystal 74.10 %; fibrous tissue 5.90 %; lipid 4.66 %; macrophage 1.23 % (Table 2). Intraclass correlation (ICC) for area were:

Table 4
Mean comparison of different plaque characteristics between 2 measurements for the same ROI i.e., intra-software mean difference (n = 42).

	Measurement 1	Measurement 2	Absolute difference	Relative difference	P value
Calcification					
Span angle (°)	23.08±14.02	23.27±14.04	−0.19±2.11	0.86 %	0.61
Thickness (mm)	0.31±0.19	0.31±0.19	0.00±0.02	1.50 %	0.47
Area (mm^2)	0.23±0.23	0.23±0.23	0.00±0.02	0.64 %	0.76
Cholesterol crystal					
Span angle (°)	6.83±2.78	6.78±2.89	0.05±0.63	0.75 %	0.65
Thickness (mm)	0.09±0.02	0.09±0.02	0.00±0.00	0.68 %	0.53
Area (mm^2)	0.01±0.005	0.01±0.006	0.00±0.001	5.34 %	0.07
Fibrous tissue					
Span angle (°)	311.95±37.01	313.37±35.02	−1.42±8.87	0.46 %	0.30
Thickness (mm)	0.90±0.19	0.90±0.19	0.00±0.01	0.20 %	0.54
Area (mm^2)	3.12±1.28	3.11±1.29	0.00±0.12	0.19 %	0.75
Cap thickness (μm)	291.29±19.08	292.62±18.79	−1.33±12.02	0.46 %	0.50
Lipid					
Span angle (°)	72.81±33.75	72.52±33.89	0.28±2.36	0.39 %	0.46
Thickness (mm)	0.57±0.16	0.56±0.16	0.00±0.02	0.89 %	0.12
Area (mm^2)	0.96±0.55	0.95±0.55	0.01±0.03	1.07 %	0.06
Macrophage					
Span angle (°)	16.07±7.73	16.14±7.70	−0.07±1.07	0.45 %	0.70
Thickness (mm)	0.11±0.03	0.11±0.03	0.00±0.00	0.59 %	0.34
Area (mm^2)	0.03±0.02	0. 03±0.01	−0.00±0.00	0.60 %	0.74

Values are mean±SD;ROI: Region of interest; Absolute difference was calculated as mean difference between measurement 1 and measurement 2; Relative difference was calculated as [1-(measurement 2/measurement 1)]x100%; P value for comparison between measurement 1 and measurement 2.

Table 5
Correlation between 2 measurements for different plaque characteristics of same region of interest i.e., intra- software correlation (n = 42).

Plaque characteristic	ICC	P value	95 % CI
Calcification			
Span angle	0.98	<0.001	0.97–0.99
Thickness	0.98	<0.001	0.97–0.99
Area	0.99	<0.001	0.98–0.99
Cholesterol crystal			
Span angle	0.97	<0.001	0.94–0.98
Thickness	0.96	<0.001	0.92–0.98
Area	0.94	<0.001	0.90–0.97
Fibrous tissue			
Span angle	0.96	<0.001	0.94–0.98
Thickness	0.99	<0.001	0.99–0.99
Area	0.99	<0.001	0.99–0.99
Minimum FCT	0.99	<0.001	0.98–0.99
Lipid			
Span angle	0.99	<0.001	0.99–0.99
Thickness	0.99	<0.001	0.98–0.99
Area	0.99	<0.001	0.99–0.99
Macrophage			
Span angle	0.99	<0.001	0.98–0.99
Thickness	0.99	<0.001	0.98–0.99
Area	0.99	<0.001	0.98–0.99

ICC: Intraclass correlation coefficient; FCT: Fibrous cap thickness. Excellent correlation was seen for all plaque characteristics.

calcification 0.86; cholesterol crystal 0.00; fibrous tissue 0.87; lipid 0.62; and macrophage 0.43 (Table 3). Inter-catheter correlation for minimum fibrous cap thickness (FCT) was good (ICC 0.70, *p*-value <0.001).

The limits of agreement for area of cholesterol crystal, fibrous tissue, calcium, lipid, and macrophage were 0.18, −0.20 mm^2; 1.14, −1.53 mm^2; 0.30, −0.34 mm^2; 0.77, −0.85 mm^2; and 0.04, −0.04 mm^2 respectively (Fig. 3). Limits of agreement for the span angle were 102.64, −120.00°; 65.00, −69.82°; 24.33, −24.02°; 48.09, −47.51°; and 14.71, −13.97° respectively and for thickness were 0.98, −1.12 mm; 0.26, −0.26 mm; 0.27, −0.26 mm; 0.23, −0.22 mm; and 0.06, −0.06 mm respectively (Supplement Fig. 1 and Fig. 2). Limits of agreement for minimum fibrous cap thickness were 137.91, −160 μm. Fig. 1 is one such example depicting good inter-catheter reproducibility by the software.

3.1.1. *Intra-software agreement*

The intra-software absolute mean difference was also statistically insignificant for all (*p* value >0.05). The intra- software relative difference for area measurements were calcification 0.64 %; cholesterol crystal 5.34 %; fibrous tissue 0.19 %; lipid 1.07 %; macrophage 0.60 % (Table 4). By intra-software measurements, there was an excellent correlation seen with ICC > 0.9 for all tissue types (Table 5).

The limits of agreement for area of cholesterol crystal, fibrous tissue, calcium, lipid, and macrophage were 0.004, −0.003 mm^2; 0.250, −0.237 mm^2; 0.052, −0.049 mm^2; 0.074, −0.053 mm^2; and 0.004, −0.004 mm^2 respectively (Fig. 4). Limits of agreement for the span angle were 1.30, −1.19°; 15.97, −18.82°; 3.94, −4.34°; 4.92, −4.34°; and 2.03, −2.18° respectively and for thickness were 0.01, −0.01 mm; 0.04, −0.03 mm; 0.06, −0.05 mm; 0.04, −0.03 mm; and 0.008, −0.007 mm respectively (Supplement Fig. 3 and Fig. 4). Limits of agreement for minimum fibrous cap thickness were 22.23, −24.89 μm.

4. Discussion

Through this study, we analyzed the reproducibility of plaque composition measurements by the Artificial Intelligence Optical Coherence Tomography software (OctPlus automated software). The main findings of our study are: a. A narrow range of agreement was demonstrated by the Bland-Altman plots for both inter-catheter and intra-software differences; b. Good inter-catheter and intra-software correlation were observed; c. The absolute mean difference of all plaque characteristics was statistically insignificant, though the inter-catheter relative difference was high for some tissue components.

Technological advances in coronary wall imaging have assisted in visualizing atherosclerotic plaque with sufficient resolution to characterize minute structures such as fibrous cap thickness (FCT). Temporal change in its measurement has been used as an imaging endpoint of longitudinal studies such as PACMAN-AMI and HUYGENS studies

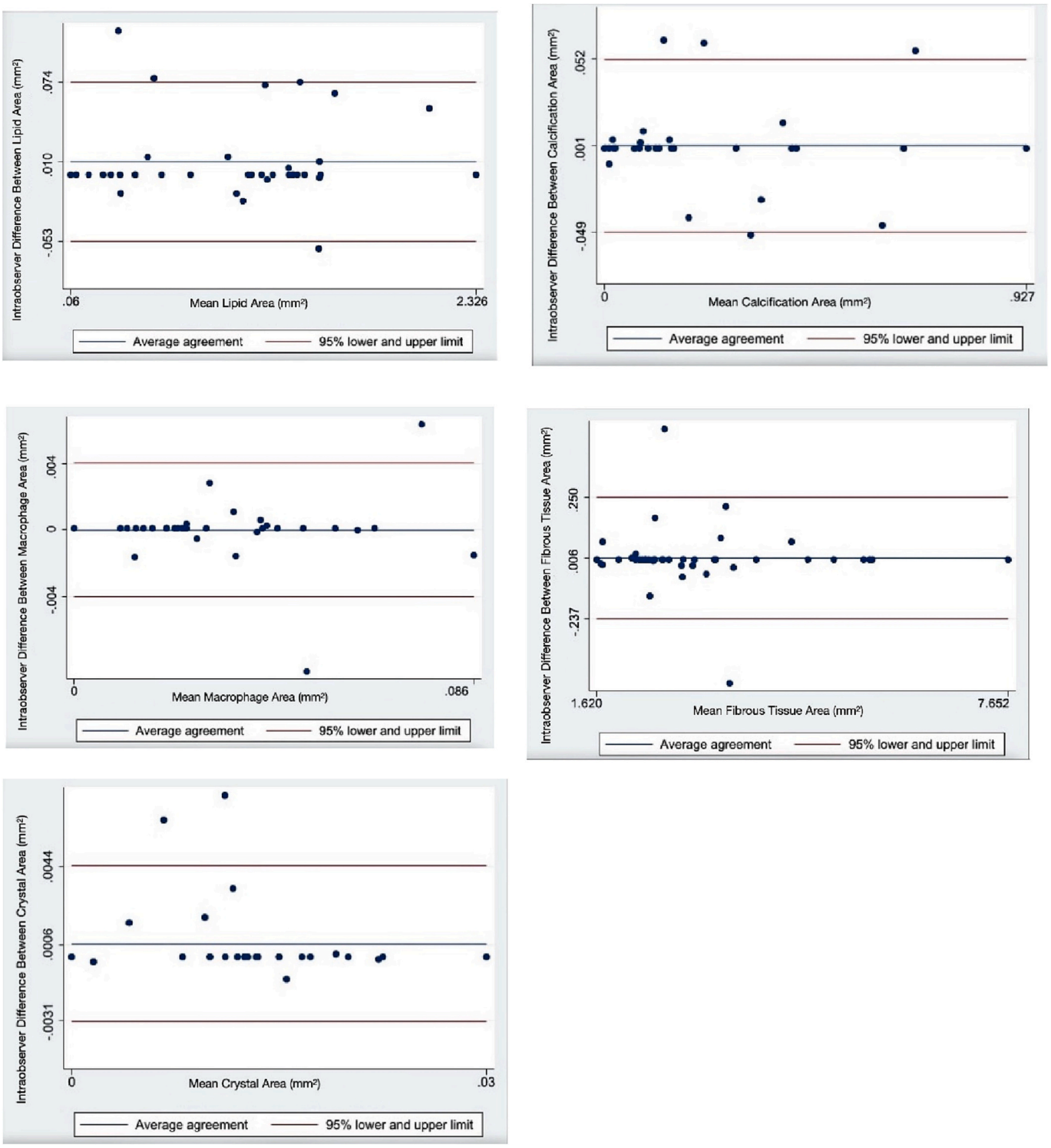

Fig. 4. Bland-Altman plots depicting the agreement between 2 different measurements by OctPlus software for same region of interest for areas of different plaque characteristics ($n = 42$).

[9,10]; in the latter study the minimum FCT change was +42.7 vs +21.5 μm, and authors reported a high agreement in the FCT evaluation. In this study, FCT measurements showed small absolute and relative mean differences in inter-catheter and intra-software measurements. This means that FCT is a reproducible endpoint which can also be measured by AI. Similarly, lipid span angle and lipid area have also been used as study endpoints due to the association between coronary plaque lipid composition and future cardiovascular events such as acute myocardial infarction and cardiac death [15,16]. In this study, both lipid arc and area showed good inter-catheter and intra-software agreement.

Several prior reports that reported reproducibility results have used visual measurements by human readers. Conversely, in our study, we used an AI-empowered OCT software. Overall, in this study, the intra-software (intra-observer – i.e., a "machine") correlation was higher than the manual interpretation done in the past. The intraclass correlation coefficient (ICC) was 0.99 for most plaque characteristics in this

study. Previously, Brown et al. reported intra-observer correlation with an ICC of 0.84 for lipid arc and 0.70 for minimum fibrous cap thickness (FCT) [17], and Radu et al. reported an ICC of 0.79 for minimum FCT [18]. Yonetsu et al. reported an intra-observer ICC of 0.97 for mean lipid arc while accessing coronary plaque characteristics in patients with diabetes mellitus and metabolic syndrome using OCT. [19] Takarada et al. checked the effect of statins on FCT and reported an intra-observer difference of 11 ± 16 μm [20], whereas the intra-observer mean difference was 1.33 ± 12.02 μm in this study. Another coronary plaque component that has been characterized by visual assessment in OCT images is calcification. Brown et al. reported an intra-observer correlation of 0.86 for calcification [17], and Gerbaud et al. showed an agreement of −2.4 ± 9.2° for calcium arc [21]. We found a better correlation and narrower limits of agreement for calcium measurements in this study.

Finally, a few points should be considered while performing longitudinal studies using this software. First, we need to be aware of the guidewire shadow. Sometimes, the guidewire shadow can obscure the plaque giving an incorrect quantification of the plaque size and characteristics (Supplement Fig. 5). Second, OCT imaging catheters are prone to non-uniform pullbacks, which impacts the determination of the size and composition of atherosclerotic plaques. Supplement fig. 6 depicts a marked difference in plaque composition for the same frame on PPCI and SPCI. The relatively high inter-catheter variability of some variables found in our study raises some caution but could be explained using above mentioned factors.

5. Limitations

The presence of a stent in the coronary vessel generates shadow on OCT images which jeopardizes the interpretation of plaque composition. Thus, cross sectional images at the stented segment were excluded from the present analysis. Hence, the severity of stenosis of the ROI analyzed is expected to be low and the software should be used with caution for a more severe lesion subset. Some previous reproducibility studies acquired both sets of images at the same time to measure inter-catheter differences [22,23]. However, the second set of OCT images was acquired at an interval of few days in this study to mimic the design of a longitudinal study. The inter-catheter measurements in our study were within acceptable limits of agreement. Some relative differences were large, especially for cholesterol crystal and macrophages since they appear mostly as an arc or a rim but the OctPlus software measures them in area. This difference could be clinically substantial, however, it was statistically insignificant in our analysis.

6. Conclusions

The present study demonstrates that the tissue characterization by the OctPlus software is acceptably reproducible. Since, the inter-catheter and intra-software reproducibility is good, investigators might use it to analyze OCT data in longitudinal studies.

CRediT authorship contribution statement

Mohil Garg: Conceptualization, Methodology, Writing – original draft, Supervision, Writing – review & editing, Data curation. **Hector M. Garcia-Garcia:** Conceptualization, Methodology, Writing – original draft, Writing – review & editing. **Andrea Teira Calderón:** Formal analysis. **Jaytin Gupta:** Data curation. **Shrayus Sortur:** Data curation. **Molly B. Levine:** Data curation. **Puneet Singla:** Data curation. **Andrea Picchi:** Resources. **Gennaro Sardella:** Resources. **Marianna Adamo:** Resources. **Enrico Frigoli:** Resources. **Ugo Limbruno:** Resources. **Stefano Rigattieri:** Resources. **Roberto Diletti:** Resources. **Giacomo Boccuzzi:** Resources. **Marco Zimarino:** Resources. **Marco Contarini:** Resources. **Filippo Russo:** Resources. **Paolo Calabro:** Resources. **Giuseppe Andò:** Resources. **Ferdinando Varbella:** Resources. **Stefano Garducci:** Resources. **Cataldo Palmieri:** Resources. **Carlo Briguori:** Resources. **Jorge Sanz Sánchez:** Formal analysis. **Marco Valgimigli:** Resources.

Declaration of competing interest

None.

Appendix A. Supplementary data

Supplementary data to this article can be found online at https://doi.org/10.1016/j.carrev.2023.07.003.

References

[1] Terashima M, Kaneda H, Suzuki T. The role of optical coherence tomography in coronary intervention. Korean J Intern Med 2012;27:1. https://doi.org/10.3904/kjim.2012.27.1.1.
[2] Prati F, Regar E, Mintz GS, Arbustini E, Di Mario C, Jang I-K, et al. Expert review document on methodology, terminology, and clinical applications of optical coherence tomography: physical principles, methodology of image acquisition, and clinical application for assessment of coronary arteries and atherosclerosis. Eur Heart J 2010;31:401–15. https://doi.org/10.1093/eurheartj/ehp433.
[3] Jang I-K, Bouma BE, Kang D-H, Park S-J, Park S-W, Seung K-B, et al. Visualization of coronary atherosclerotic plaques in patients using optical coherence tomography: comparison with intravascular ultrasound. J Am Coll Cardiol 2002;39:604–9. https://doi.org/10.1016/s0735-1097(01)01799-5.
[4] Kim S-J, Lee H, Kato K, Yonetsu T, Xing L, Zhang S, et al. Reproducibility of in vivo measurements for fibrous cap thickness and lipid arc by OCT. JACC Cardiovasc Imaging 2012;5:1072–4. https://doi.org/10.1016/j.jcmg.2012.04.011.
[5] Koskinas KC, Ughi GJ, Windecker S, Tearney GJ, Räber L. Intracoronary imaging of coronary atherosclerosis: validation for diagnosis, prognosis and treatment. Eur Heart J 2016;37. https://doi.org/10.1093/eurheartj/ehv642. 524-535a-c.
[6] Montarello NJ, Singh K, Sinhal A, Wong DTL, Alcock R, Rajendran S, et al. Assessing the impact of colchicine on coronary plaque phenotype after myocardial infarction with optical coherence tomography: rationale and design of the COCOMO-ACS study. Cardiovasc Drugs Ther 2022;36:1175–86. https://doi.org/10.1007/s10557-021-07240-9.
[7] Habara M, Nasu K, Terashima M, Ko E, Yokota D, Ito T, et al. Impact on optical coherence tomographic coronary findings of fluvastatin alone versus fluvastatin + ezetimibe. Am J Cardiol 2014;113:580–7. https://doi.org/10.1016/j.amjcard.2013.10.038.
[8] Komukai K, Kubo T, Kitabata H, Matsuo Y, Ozaki Y, Takarada S, et al. Effect of atorvastatin therapy on fibrous cap thickness in coronary atherosclerotic plaque as assessed by optical coherence tomography: the EASY-FIT study. J Am Coll Cardiol 2014;64:2207–17. https://doi.org/10.1016/j.jacc.2014.08.045.
[9] Nicholls SJ, Kataoka Y, Nissen SE, Prati F, Windecker S, Puri R, et al. Effect of Evolocumab on coronary plaque phenotype and burden in statin-treated patients following myocardial infarction. JACC Cardiovasc Imaging 2022;15:1308–21. https://doi.org/10.1016/j.jcmg.2022.03.002.
[10] Räber L, Ueki Y, Otsuka T, Losdat S, Häner JD, Lonborg J, et al. Effect of Alirocumab added to high-intensity statin therapy on coronary atherosclerosis in patients with acute myocardial infarction: the PACMAN-AMI randomized clinical trial. JAMA 2022;327:1771–81. https://doi.org/10.1001/jama.2022.5218.
[11] Pulse-Imaging. Available at http://en.pulse-imaging.com. Last accessed on Jan 17, 2023.
[12] Chu M, Jia H, Gutiérrez-Chico JL, Maehara A, Ali ZA, Zeng X, et al. Artificial intelligence and optical coherence tomography for the automatic characterisation of human atherosclerotic plaques. EuroIntervention 2021;17:41–50. https://doi.org/10.4244/EIJ-D-20-01355.
[13] Gutiérrez-Chico JL, Chen Y, Yu W, Ding D, Huang J, Huang P, et al. Diagnostic accuracy and reproducibility of optical flow ratio for functional evaluation of coronary stenosis in a prospective series. Cardiol J 2020;27:350–61. https://doi.org/10.5603/CJ.a2020.0071.
[14] Available at https://clinicaltrials.gov/ct2/show/NCT01433627. Last accessed on Jan 17, 2023.
[15] Prati F, Romagnoli E, Gatto L, La Manna A, Burzotta F, Ozaki Y, et al. Relationship between coronary plaque morphology of the left anterior descending artery and 12 months clinical outcome: the CLIMA study. Eur Heart J 2020;41:383–91. https://doi.org/10.1093/eurheartj/ehz520.
[16] Stone GW, Maehara A, Lansky AJ, de Bruyne B, Cristea E, Mintz GS, et al. A prospective natural-history study of coronary atherosclerosis. N Engl J Med 2011;364:226–35. https://doi.org/10.1056/NEJMoa1002358.
[17] Brown AJ, Jaworski C, Corrigan JP, de Silva R, Bennett MR, Mahmoudi M, et al. Optical coherence tomography imaging of coronary atherosclerosis is affected by intraobserver and interobserver variability. J Cardiovasc Med 2016;17:368–73. https://doi.org/10.2459/JCM.0000000000000304.
[18] Radu MD, Yamaji K, García-García HM, Zaugg S, Taniwaki M, Koskinas KC, et al. Variability in the measurement of minimum fibrous cap thickness and reproducibility of fibroatheroma classification by optical coherence tomography using manual versus semi-automatic assessment. EuroIntervention 2016;12:e987–97. https://doi.org/10.4244/EIJV12I8A162.

[19] Yonetsu T, Kato K, Uemura S, Kim B-K, Jang Y, Kang S-J, et al. Features of coronary plaque in patients with metabolic syndrome and diabetes mellitus assessed by 3-vessel optical coherence tomography. Circ Cardiovasc Imaging 2013;6:665–73. https://doi.org/10.1161/CIRCIMAGING.113.000345.

[20] Takarada S, Imanishi T, Kubo T, Tanimoto T, Kitabata H, Nakamura N, et al. Effect of statin therapy on coronary fibrous-cap thickness in patients with acute coronary syndrome: assessment by optical coherence tomography study. Atherosclerosis 2009;202:491–7. https://doi.org/10.1016/j.atherosclerosis.2008.05.014.

[21] Gerbaud E, Weisz G, Tanaka A, Kashiwagi M, Shimizu T, Wang L, et al. Multi-laboratory inter-institute reproducibility study of IVOCT and IVUS assessments using published consensus document definitions. Eur Heart J Cardiovasc Imaging 2016;17:756–64. https://doi.org/10.1093/ehjci/jev229.

[22] Rodriguez-Granillo GA, Vaina S, García-García HM, Valgimigli M, Duckers E, van Geuns RJ, et al. Reproducibility of intravascular ultrasound radiofrequency data analysis: implications for the design of longitudinal studies. Int J Cardiovasc Imaging 2006;22:621–31. https://doi.org/10.1007/s10554-006-9080-0.

[23] Gaster AL, Korsholm L, Thayssen P, Pedersen KE, Haghfelt TH. Reproducibility of intravascular ultrasound and intracoronary Doppler measurements. Catheter Cardiovasc Interv 2001;53:449–58. https://doi.org/10.1002/ccd.1202.